Adsorption
https://doi.org/10.1007/s10450-019-00096-4

Highly efficient removal of heavy metals from waters by magnetic chitosan-based composite

Marcos E. Peralta[1] · Roberto Nisticò[2] · Flavia Franzoso[3] · Giuliana Magnacca[3,4] · Laura Fernandez[5] · Maria E. Parolo[6] · Emilio García León[6] · Luciano Carlos[1]

Received: 28 August 2018 / Revised: 10 February 2019 / Accepted: 22 April 2019

Abstract

Magnetic chitosan composite (MCC) made by chitosan matrix embedding magnetite/maghemite were developed for the removal of toxic Cu(II), Pb(II), and Ni(II) from water. Thermogravimetric (TGA) and Zeta potential analyses showed that MCC contains ca. 50 wt % of chitosan and presents a value of isoelectric point (pH_{IEP}) around 8-8.5. The magnetization curve revealed a saturation magnetization of 12 emu g^{-1}, which indicates that MCC can be easily recovered by magnetic separation. Adsorption of the heavy metals to MCC reached equilibrium within 120 min with maximum uptakes of 108.9 mg g^{-1}, 216.8 mg g^{-1} and 220.9 mg g^{-1} for Ni(II), Cu(II) and Pb(II), respectively. The results show that the amino and hydroxyl functional groups of chitosan are involved in the adsorption process. The reported adsorption capacity from organic pollutants, such as hydrocarbons, along with the high adsorption capacity shown for heavy metals, point out MCC being a promising versatile adsorbent for wastewater treatments.

Keywords Adsorption · Chitosan · Heavy metal · Magnetic material · Water treatment

1 Introduction

The discharge of heavy metals into natural waters is an important environmental issue (USEPA 2008). The major sources of heavy metal pollutions derive from industrial activities including mining, metal plating, oil refining, electronic devices manufacturing, the production of chemicals, petrochemicals, paints, fertilizers, pulp and paper, textiles, leather, and pesticides (Azzam et al. 2016). Wastewater from these industries commonly contains Cu(II), Ni(II), Pb(II) and other metals and the presence of these species is of a great concern because they are toxic to human health and the environment (Ahmad and Mirza 2018). The World Health Organization (WHO) set the maximum allowed limit of Pb(II), Ni(II) and Cu(II) in drinking water at 0.01, 0.07 and 2 mg L^{-1}, respectively (World Health Organization 2011). Taking this into account, the selection of an effective procedure of remediation from heavy metals is required. Several methods, including ion exchange, adsorption, precipitation and membrane processes have been proposed to treat surface and groundwater polluted with heavy metals (Lin and Sen-Gupta 2009; Modin et al. 2011). Among these, adsorption is a relatively effective and economical method for the

Electronic supplementary material The online version of this article (https://doi.org/10.1007/s10450-019-00096-4) contains supplementary material, which is available to authorized users.

✉ Luciano Carlos
luciano.carlos@probien.gob.ar

[1] Instituto de Investigación y Desarrollo en Ingeniería de Procesos, Biotecnología y Energías Alternativas, PROBIEN (CONICET-UNCo), Buenos Aires 1400, 8300 Neuquén, Argentina

[2] Department of Applied Science and Technology DISAT, Polytechnic of Torino, C.so Duca degli Abruzzi 24, 10129 Turin, Italy

[3] Department of Chemistry, University of Torino, Via P. Giuria 7, 10125 Turin, Italy

[4] NIS Interdepartmental Centre, Via P. Giuria 7, 10125 Turin, Italy

[5] Facultad de Ingeniería, Universidad Nacional del Comahue, Buenos Aires 1400, 8300 Neuquén, Argentina

[6] Instituto de Investigación en Toxicología Ambiental y Agrobiotecnología, CITAAC (CONICET-UNCo), Facultad de Ingeniería, Universidad Nacional del Comahue, Buenos Aires 1400, 8300 Neuquén, Argentina

Published online: 30 April 2019

removal of metals from waters. Although activated carbon has been widely used as one of the most popular sorbents for the removal of various pollutants, there is an increasing interest in developing alternative sorbents which are cost-effective, sustainable, and highly efficient in the removal of metal ions in waters (Babel 2003; Musso et al. 2014). In this context, there has been a growing interest and research progress on the use of bio-based materials, derived from low-cost and environmentally friendly source. Chitosan, an amino polysaccharide derived from chitin (component of lobster and shrimp shells, crabs, cuticles of insects, beaks and cuttlebones, squid and octopus radulae, and cell walls of some fungi), have been used in biotechnology as well as in water treatments (Boddu et al. 2008; Cho et al. 2012; Nisticò 2017a). Several publications describe the efficacy of chitosan sorbents in the removal of several pollutants such as metals, dyes, and phenols (Jin et al. 2017; Nguyen et al. 2016; Yang et al. 2016). Laus et al. (2010) studied the adsorption and desorption of Cu(II), Cd(II) and Pb(II) ions using chitosan crosslinked with epichlorohydrin-triphosphate. Li et al. (2015) reported the adsorption of heavy metal ions on chitosan/sulfhydryl functionalized graphene oxide composites. In order to improve the adsorption capacity and selectivity on metal ions, a number of chitosan derivatives has been obtained by grafting new functional groups through a crosslinked chitosan backbone (Li et al. 2011; Wang and Wang 2016; Zhu et al. 2012). However, the use of such materials in aqueous medium presents some limitations in their recovery, since they require complex separation procedures. The preparation of easily recoverable adsorbing materials, such as magnetic-response one, is set out in the literature to solve this issue (Magnacca et al. 2014; Nisticò 2017b; Su 2017). Magnetic chitosan composites (MCC in the following), consisting in dispersed magnetic particles in a chitosan polymer matrix, are interesting active phases exhibiting good sorption capacity towards various pollutants in aqueous solution (Li et al. 2016; Liang et al. 2017; You et al. 2018). In previous studies, we investigated the adsorption capacity of chitosan derived magnet-sensitive materials versus polycyclic aromatic hydrocarbons and arsenic species from aqueous solutions (Nisticò et al. 2018; Nisticò et al. 2017). Our findings highlight the versatility of these materials in the removal of different classes of pollutants, encouraging their applications in wastewater treatments.

Based on these considerations and with the aim of expanding the range of pollutants to be removed, in the present work chitosan-magnetite nanocomposite has been produced and tested for the removal of Cu(II), Ni(II) and Pb(II) ions from water. A deep physicochemical characterization of the chitosan-based magnetic material was carried out. Sorption properties varying several operational conditions, such as contact time, adsorbent dosage, pH solution, initial heavy metal concentration, presence of soluble organic matter and competitive ions, were studied. Adsorbent regeneration and reuse were also analysed.

2 Materials and methods

2.1 Materials

$FeCl_3$ (purity ≥ 98%) and $FeSO_4 \times 7H_2O$ (purity ≥ 99.5%) were purchased from Fluka Chemika. Partially N-deacetylated chitosan (DD = 75–85%) of medium molecular weight (Mv = 190–310 kDa) with Brookfield viscosity of 200–800 cps (from crab shells) was purchased from Sigma-Aldrich. Heavy metal standards of Copper, Nickel, and Lead for atomic absorption spectrophotometric analysis (AAS) (1000 mg L^{-1}, Sigma-Aldrich) were used for adsorption experiments. Leonardite humic substances standard were obtained from International Humic Substances Society (IHSS). Other reagents used were ammonium hydroxide solution (NH_3 essay 28–30%, E. Merck), hydrochloric acid (HCl, conc. 37 wt%, Fluka Chemika), nitric acid (HNO_3 conc. 70 wt%, Mallinckrodt). All aqueous solutions for adsorption experiments were prepared using ultrapure water Millipore Milli-Q™. All chemicals were used without further purification.

2.2 Synthesis of MCC

Magnetic chitosan composite (MCC) was prepared according to the one-step procedure reported in the literature (Cesano et al. 2015). Briefly, $FeCl_3$ (3.7 g) and $FeSO_4 \times 7H_2O$ (4.17 g) salts were dissolved in 100 mL of deionized water at room temperature and heated up to 90 °C. As soon as the desired temperature was reached, 10 mL of ammonium hydroxide (25 vol%), and 50 mL of a previously prepared chitosan aqueous solution in a weak acid environment (3 wt%) were added. The mixture was stirred at 90 °C for 30 min. The obtained precipitate was separated using a neodymium magnet, washed with deionized water and oven-dried at 80 °C overnight. For the sake of comparison, also a bare magnetite/maghemite reference material was synthesized following the same procedure without chitosan addition.

2.3 Characterization

Fourier transform infrared (FTIR) spectra were obtained by using a Bruker Vector 22 spectrophotometer equipped with Globar source and DTGS detector on KBr pellets. The spectrum was recorded in transmission mode with 128 scans at 4 cm^{-1} resolution in the $4000 - 400$ cm^{-1} range. X-ray diffraction (XRD) patterns were recorded by using a X'Pert

PRO MPD diffractometer from PANalytical with Cu anode (45 kV, 40 mA) in a Bragg–Brentano geometry on a spinner sample holder (60 rpm). The XRD pattern acquisition was performed in the range of 2θ value between 10° and 70°. Thermogravimetric analyses were performed by a Rigaku Evo Plus II TGA model operating at high resolution with ramp 10 °C min^{-1} from room temperature to 1000 °C in air flow (100 cm^3 min^{-1}). High-resolution transmission electron microscopy (HR-TEM) measurements were performed on a JEOL JEM 3010 instrument (300 kV) equipped with a LaB6 filament. The zeta potential (ζ) was measured on aqueous dispersions of MCC at different pH values by means of a Malvern Instruments zetasizer. Magnetization measurements were carried out by using a LakeShore 7404 vibrating sample magnetometer. The hysteresis loop of all samples was registered at room temperature with a magnetic field sweeping between −20,000 and 20,000 Oe.

2.4 Adsorption experiment

Adsorption of heavy metals on MCC adsorbents was investigated performing batch experiments under continuous shaking at constant temperature (25 °C). Stock solutions of the heavy metals (100 mg L^{-1} in 3% HNO_3) were prepared from standard solutions. In a typical procedure, MCC was dispersed by ultrasound (10 min) in water. Then, a volume of stock heavy metal solutions was spiked on the MCC dispersion and the pH of the system was adjusted with HCl or NaOH solutions to the desired value. The mixture was shaken (160 rpm) in closed flask at 25 °C for a certain time. Then, the magnetic nanocomposites were separated from the mixture by a neodymium magnet and the residual heavy metals concentration in the supernatant was determined by using a Perkin Elmer A200 atomic absorption spectrophotometer (AAS). Before the AAS analyses, the samples were filtered with a Nylon 0.45 µm filter. The uptake at a certain time, q_t (mg g^{-1}), and the % removal were calculated by the following equations:

$$q_1 = \frac{(C_0 - C_t) \times V}{m} \tag{1}$$

$$\%\,\text{Removal} = \frac{(C_0 - C_t) \times 100}{C_0} \tag{2}$$

where C_0 and C_t are the heavy metal concentration (mg L^{-1}) at time 0 min and t min, respectively, V is the volume (L) of the solution and m is the mass (g) of the adsorbent. All experiments were carried out in triplicate and data presented are the mean values from these independent experiments.

The adsorption capacities of MCC to Cu(II), Ni(II) and Pb(II) were measured individually at pH 6.0 with 50 mg L^{-1} of MCC varying metal concentration (1–20 mg L^{-1}). The data were fitted applying Langmuir, Freundlich and Dubinin–Kaganer–Radushkevich (DKR) adsorption isotherms. The Langmuir model is based on the assumption of monolayer adsorption onto adsorbent surface, finite capacity adsorption for adsorbate, and the occupation of a metal ion on one site. The Langmuir model is expressed as:

$$q_e = \frac{q_{\max} K_L C_e}{1 + K_L C_e} \tag{3}$$

where q_e is the adsorbed heavy metal at equilibrium, C_e is the heavy metal concentration (mg L^{-1}), q_{max} is the maximum adsorption capacity and K_L is the equilibrium constant (L mg^{-1}).

The Freundlich isotherm suggests that the adsorption phenomenon occurs on heterogeneous surfaces (Lasheen et al. 2016) and assumes that the surface sites of the adsorbent have different binding energies. Freundlich adsorption isotherm is described as:

$$q_e = K_F C_e^{1/n} \tag{4}$$

K_F is the Freundlich constant ((mg g^{-1})(L mg^{-1})$^{1/n}$) indicative of the relative adsorption capacity of the adsorbent and n is the degree of dependence of adsorption with equilibrium concentration and is related to the sorption intensity.

The DKR isotherm helps in predicting the nature of adsorption by determining the apparent energy of adsorption. This model does not assume a homogenous surface or constant sorption potential. DKR isotherm is expressed as:

$$q_e = X_{max} \exp\left(-\beta\left[RT \ln\left(1 + \frac{1}{C_e}\right)\right]^2\right) \tag{5}$$

where X_{max} is the maximum sorption capacity, β (mol^2 kJ^{-2}) is the activity coefficient related to mean sorption energy, R (kJ $kmol^{-1}$ K^{-1}) is the gas constant and T is the absolute temperature (K). E is defined as the free energy change (kJ mol^{-1}), which is required to transfer 1 mol of ions from solution to the solid surfaces and is calculated as shown in Eq. 6.

$$E = \frac{1}{\sqrt{2\beta}} \tag{6}$$

The magnitude of E is useful for estimating the mechanism of the adsorption process. Adsorption is dominated by chemical ion-exchange process if E is in the range of 8–16 kJ mol^{-1}, whereas in the case of E < 8 kJ mol^{-1} the adsorption is a simple physical process (Lasheen et al. 2016).

2.5 Regeneration and reuse of MCC nanocomposites

Several adsorption and regeneration cycles were performed in order to test the MCC reusability. For the adsorption stage, 30 mg of MCC was contacted with 120 mL of 2 mg L^{-1} Cu(II) at pH 6 and then shaken for 2 h. After magnetic separation, an aliquot was withdrawn for the determination of Cu(II) equilibrium concentration and the remained supernatant was discarded. Later, for the regeneration stage, 120 mL of HCl solution at pH 3 was added to the MCC and the dispersion was shaking for 2 h. The solid was magnetically separated and the Cu(II) amount desorbed was determined in the supernatant. The regenerated MCC was then reused for subsequent Cu(II) adsorption experiments.

3 Results and discussion

3.1 Characterization of MCC

XRD pattern of MCC is shown in Fig. S1 in the Online Resource 1. The reflections at 2θ = 30.1°, 35.4°, 43.0°, 53.9°, 57.2° and 63° can be associated with (220), (311), (400), (422), (511) and (440) X-ray diffraction planes of magnetite (card number 00-019-0629, ICCD Database) and/or maghemite (card number 00-039-1346, ICCD Database). These two phases cannot be distinguished by means of XRD data, but the presence of maghemite is expected to be due to the topotactic oxidation of magnetite into maghemite (Cesano et al. 2015). Furthermore, the reflection at 2θ = 20.1° can be attributed to chitosan (Li et al. 2015). The narrow diffraction peaks at 2θ = 33.0°, 47.3° and 58.6° associated to (110), (200) and (211) ammonium chloride crystalline plane (card number 01-073-0363, ICCD Database) revealed the presence of synthesis impurities not eliminated after material washing. HR-TEM images revealed the presence of crystalline spherical nanoparticles dispersed in an amorphous organic phase (Fig. S2, in the Online Resource 1). The FTIR spectrum of MCC evidenced the chitosan skeletal fingerprint (Fig. 1). Specifically, C–O and C–O–C stretching vibration modes of glycosidic functional groups between 1160 and 900 cm^{-1} and amide group vibration bands between 1750 and 1600 cm^{-1} (Mano et al. 2003; Neeraj et al. 2016; Nisticò et al. 2017; Zhang et al. 2013). The vibration modes at 567 and 625 cm^{-1}, assigned to Fe–O stretching, confirms the formation of the iron oxide phase in MCC nanocomposites (Magnacca et al. 2014).

TGA curves of MCC in oxidant atmosphere are shown in Fig. 2. The mass loss in the lowest interval of temperature (30–160 °C) corresponds to the moisture content in the sample (Corazzari et al. 2015). Between 200 and 500 °C, the largest mass loss attributed to the chitosan degradation

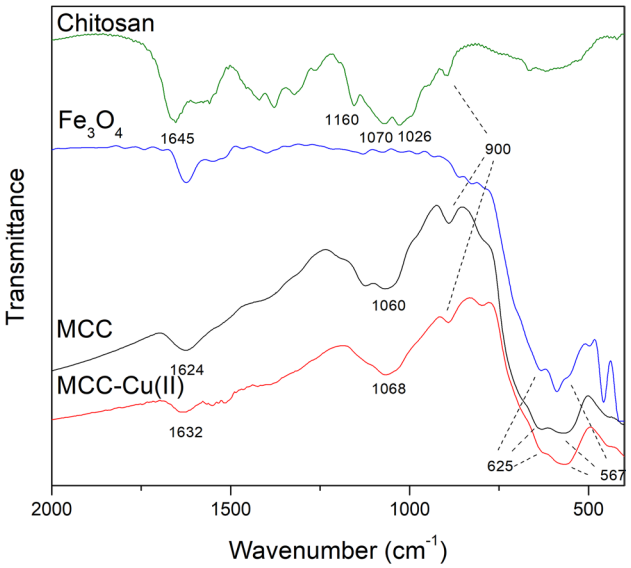

Fig. 1 Transmittance FTIR spectra of magnetite/maghemite reference (Fe_3O_4), chitosan, MCC nanocomposite and MCC-Cu (II) adsorption complex

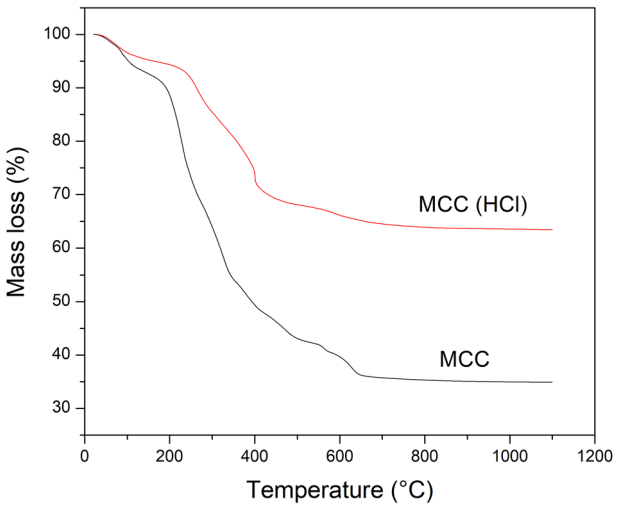

Fig. 2 TGA curves of MCC and MCC after acid treatment

takes place. From the TGA analysis, it was estimated that the average chitosan content is ca. 52.5%. The mass variation between 500 and 800 °C is attributable to the presence of iron oxide in the nanocomposite (Li et al. 2008).

Figure 3 shows zeta potential (ζ) values of bare magnetite and MCC (100 mg L^{-1}) measured in 10^{-2} M KCl aqueous solutions at different pHs (3 – 10, adjusted with KOH or HCl). The isoelectric point (pH_{IEP}) of Fe_3O_4 was 7.2, which is close to that reported in the literature (Chang and Chen 2005), whereas for MCC increased to a value of 8.0. It is worth mentioning that the lower negative potential of MCC than the magnetite/maghemite reference is in agreement

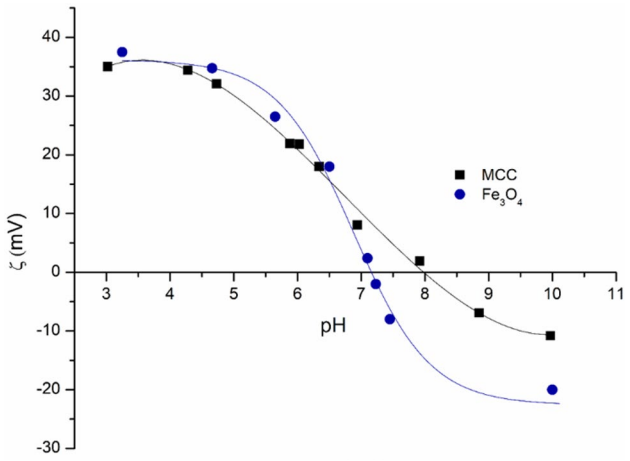

Fig. 3 Zeta potential of magnetite/maghemite reference (Fe_3O_4) and MCC at different pH values

with iron oxide nanoparticles dispersed in the chitosan matrix, since chitosan is less negative than Fe_3O_4 at pHs > 7 (Arias et al. 2012).

Figure S3, in the Online Resource 1, reports the magnetization curves obtained for the MCC and magnetite/maghemite reference nanoparticles at 300 K. Both materials exhibited superparamagnetic characteristics (including zero coercivity and remanence) with a saturation magnetization (Ms) of 64 emu g^{-1} for magnetite/maghemite and 12 emu g^{-1} for MCC. Taking into account that MCC bears 52.5% of chitosan (TGA results) and hypothesizing that the magnetization should decrease only by the amount of chitosan per grams of MCC, it should be expected a value of Ms close to 30.4 emu g^{-1}. The lower Ms value obtained for MCC (i.e. 12 emu g^{-1}) could be accounted for the quenching of surface moments in the nanocomposites induced by the presence of non-magnet-sensitive species, such as chitosan (Kim et al. 2003). Nevertheless, separation of MCC from its aqueous dispersions can be easily ended in a few minutes by applying an external magnetic field.

3.2 Adsorption experiments

Preliminary experiments were performed in order to evaluate the potential application of MCC in the adsorption of heavy metals. First, the adsorption kinetics of each heavy metal were carried out to understand the adsorption behaviour of the prepared nanomaterial. Three adsorption kinetic models (pseudo-first order, pseudo-second order and intraparticle diffusion) were selected to estimate the adsorption mechanism and quantify the extent of uptake in the adsorption process. The three equations employed to model the sorption data over the entire time range could be generally expressed as follows (Ho 2006; Qiu et al. 2009):

Table 1 Kinetic results for the removal of Cu(II), Pb(II) and Ni(II) by MCC

Kinetic models	Pb(II)	Cu(II)	Ni(II)
Pseudo-first order			
k_1 (min^{-1})	0.024	0.034	0.021
q_e (mg g^{-1})	1.55	1.87	0.84
R^2	0.91	0.95	0.84
Pseudo-second order			
k_2 (g mg^{-1} min^{-1})	0.035	0.030	0.026
q_e (mg g^{-1})	2.15	2.05	1.64
R^2	0.99	0.99	0.98
Intraparticle diffusion			
k_{p1} (mg g^{-1} $min^{-1/2}$)	0.153	0.181	0.174
C	0.21	0.14	0.03
R^2	0.83	0.95	0.99
k_{p2} (mg g^{-1} $min^{-1/2}$)	0.016	0.018	0.008
C	1.76	1.63	1.32
R^2	0.40	0.42	0.30

$$\text{pseudo} - \text{first order}: \ln(q_e - q_t) = \ln(q_e) - k_1 t \quad (7)$$

$$\text{pseudo} - \text{second order}: \frac{1}{q_t} = \frac{1}{k_2 q_e^2} - \frac{t}{q_e} \quad (8)$$

$$\text{intraparticle diffusion}: q_t = k_p t^{1/2} + C \quad (9)$$

where q_t is the adsorption capacity at time t (mg g^{-1}), q_e is the equilibrium adsorption capacity (mg g^{-1}), k_1 (min^{-1}) is the pseudo-first order rate constant, k_2 (g mg^{-1} min^{-1}) is the pseudo-second order rate constant, k_p is the intraparticle diffusion rate constant (mg g^{-1} $min^{1/2}$) and C is the intercept. The kinetic studies for Cu(II), Ni(II) and Pb(II) adsorption onto the MCC were carried out by varying the contact time from 0 to 4 h (Fig. S4, in the Online Resource 1). The adsorption capacity increased markedly at the early 60 min and then slowly increased until the adsorption equilibrium was reached after approximately 120 min. Figures S5–S7, in the Online Resource 1, display the fits of the kinetic models over the experimental data. The kinetic parameters and the coefficient of determination (R^2) values obtained for each heavy metal from the three kinetic models are listed in Table 1. The data for Cu(II), Pb(II) and Ni(II) suggest that the pseudo-second order model is the most appropriate for these metals, as their R^2 are the highest and the calculated adsorption capacities (q_e) are in agreement with the experimental values. This indicates that the rate-limiting step of the adsorption mechanism is the adsorption reaction on the surface of adsorbent (Liu 2008). On the other hand, intraparticle diffusion model could bring complementary information for the diffusion mechanism. Plots of q_t versus $t^{1/2}$

(Fig. S7, in the Online Resource 1) have two linear regions, indicating different stages in the adsorption process. The first stage presented a large slope (k_{p1}, Table 1), which might be due to the mass transfer from the solution to the outer surface of MCC, whereas the subsequent second linear region indicates a slower adsorption stage (k_{p2}, Table 1) which could be ascribed to the intra-particle diffusion of the metal ions to the inner surface of MCC. Besides, both lines of the two stages do not pass through the origin, which indicates that the intra-particle diffusion is not the only mechanism controlling the adsorption of Pb(II), Cu(II) and Ni(II) onto MCC. A similar diffusion mechanism was reported for the adsorption of heavy metals onto other chitosan-based sorbents (Ibrahim et al. 2019; Kongarapu et al. 2018).

From the kinetic results the equilibrium adsorption capacities follow the order Pb(II) > Cu(II) > Ni(II). The difference in the adsorption extent among the tested heavy metals could be accounted for the covalent index, which reflects the degree of covalent interactions in the metal ligand complex relative to ionic interactions (Mokhtari and Keshtkar 2016; Owsianiak et al. 2014). In general, biosorbents usually have a higher affinity for metal ions with larger covalent index (Dragan and Loghin 2018; Martín-Lara et al. 2016). The covalent index, calculated as the product of electronegativity of a metal ion in the crystal phase and its ionic radius, are 3.89, 3.39 and 2.62 for Pb(II), Cu(II) and Ni(II), respectively (Owsianiak et al. 2014). This trend agrees with the order of adsorption capacity of Pb(II), Cu(II) and Ni(II), suggesting that the adsorption capacity tendency could be correlated with the concept of covalent index.

Figure 4a, b and c show the adsorption isotherms of Cu(II), Pb(II) and Ni(II) on MCC. The adsorption parameters of the Langmuir, Freundlich and DKR isotherm models were analysed using nonlinear regression, and the results are displayed in Fig. 4a, b, c and Table 2. It can be seen that R^2 of the Langmuir isotherm model is better than the corresponding R^2 values from the Freundlich and DKR isotherm models, suggesting that the adsoprtion behaviors of Cu(II), Pb(II) and Ni(II) could be well described by the Langmuir model. Consequently, this result suggests a homogeneous distribution of the surface sites active towards metal adsorption. This is in agreement with previous works on chitosan composites describing adsorption isotherms through Langmuir model (Chang and Chen 2005; Cho et al. 2012). Pb(II) showed the highest maximum adsorption capacity among the tested metals. A comparison of the adsorption capacity (q_{max}) of MCC towards heavy metals with other adsorbing materials reported in the literature (Table 3) shows that MCC presents in most cases the highest adsorption capacities ever observed. On the other hand, the E values derived from DKR (8.77–12.91 kJ mol^{-1}) are in the energy range of chemical ion exchange reactions. To further gain insight on the adsorption mechanism, MCC was analysed by FTIR

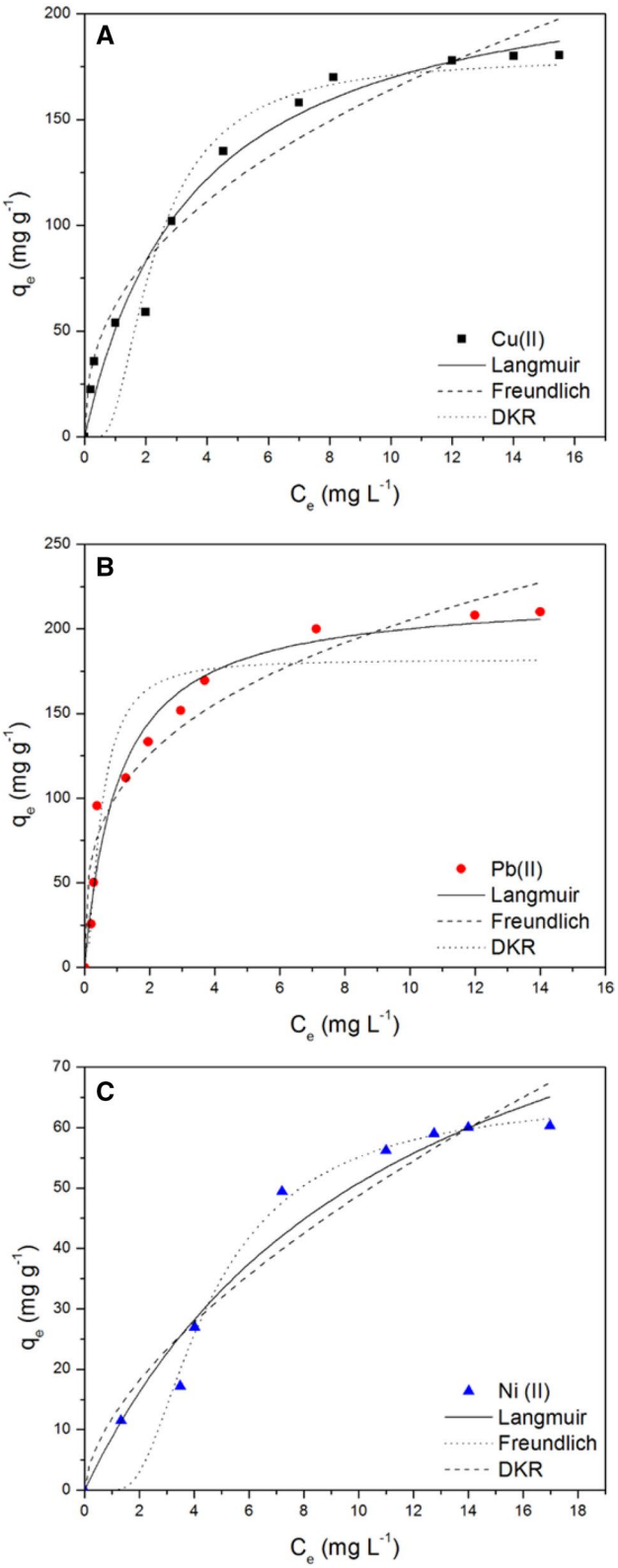

Fig. 4 Adsorption isotherms of heavy metals on MCC. **a** Cu(II), **b** Pb(II) and **c** Ni(II). [MCC] = 50 mg L^{-1}, pH = 6, contact time = 3 h and T = 25 °C

Table 2 Freundlich, Langmuir and DKR isothermal sorption parameters for the adsorption of Ni(II), Cu(II) and Pb(II) by MCC

Isotherm parameters	Pb(II)	Cu(II)	Ni(II)
Freundlich			
1/n	0.30	0.42	0.61
K_F (mg g^{-1})	102.06	62.03	11.88
R^2	0.94	0.96	0.94
Langmuir			
q_{max} (mg g^{-1})	220.9	216.8	108.9
K_L (L mg^{-1})	0.96	0.36	0.09
R^2	0.96	0.99	0.96
DKR			
X_{max} (mg g^{-1})	198.8	179.7	65.3
E (kJ mol^{-1})	12.91	11.32	8.77
R^2	0.86	0.97	0.94

after Cu(II) adsorption. The experiment was performed at pH lower than pH_{IEP} of MCC, where the $–NH_2$ groups of chitosan are protonated. In this condition, the adsorption could occur by replacing H^+ with a metal ion through an ion exchange process (Horst et al. 2016). The FTIR spectrum of MCC after Cu(II) adsorption was recorded to identify the chemical groups possibly involved in Cu(II) capture (Fig. 1). Modification of the FTIR spectrum in the range 1450–1550 cm^{-1} were observed after Cu(II) adsorption. This can be ascribed to the deformation vibration in $–NH_2$, suggesting that nitrogen atoms can be involved in Cu(II) ions adsorption. Besides, both 1060 cm^{-1} and 1624 cm^{-1} absorption bands (C–O and amide groups) shifts to higher wavenumbers, indicating that the oxygen atoms in the MCC structure could also interact with Cu(II) ions.

Since the three heavy metals showed similar adsorption behaviour, Cu(II) was selected as a model to evaluate the effect of the experimental conditions (i.e. pH, adsorbate loading, water matrix, etc.) on the adsorption capacity. Figure 5a shows the effect of the pH on the Cu(II) adsorption capacity of MCC. The data exhibit low Cu(II) adsorption capacity (< 15%) at pH values lower than 3, while at pH values higher than 4, the Cu(II) removal significantly increased to near 85%. The low Cu(II) uptake at pH lower than 3 is probably a result of a chitosan solubilization in the acidic environment (Arias et al. 2012). In order to evaluate this hypothesis, TGA analysis on the MCC previously dispersed in HCl solution (pH 3) for 3 h was performed (Fig. 2). This analysis evidences the presence of 25% of chitosan on MCC vs. the original 52.5%, indicating that half of the chitosan present in the material undergoes solubilisation. Moreover, it is important to notice that at pH > 7, part of Cu(II) ions starts to precipitate as copper hydroxides and copper oxides (Gao et al. 2016), and this can affect the results of the measurement suggesting a false increase of Cu(II) removal. Considering these aspects, we select the pH 6 for the adsorption assays as the best compromise to have the higher removal percentage without a significant chitosan-solubilization and/or Cu-precipitation. Figure 5b displays the effect of the MCC loading on the removal of Cu(II). Results show that the higher the MCC loaded, the higher the Cu(II) removal, obtaining 95% removal with 500 mg L^{-1} of adsorbent.

In natural water samples, competitive complexation of heavy metal ions with water constituents (e.g., inorganic and

Table 3 Removal of heavy metals from waters using different adsorbents

Heavy metal	Adsorbent	q_{max} (mg g^{-1})	Reference
Pb(II)	Activated carbon	21.4	(Mouni et al. 2011)
	Na-Montmorillonite	35.6	(Zhu et al. 2011)
	Fe_3O_4@SiO_2-NH_2	243.9	(Wang et al. 2015)
	Fe_3O_4-chitosan	63.3	(Tran et al. 2010)
	Fe_3O_4-chitosan films	114.9	(Lasheen et al. 2016)
	This work	220.9	
Cu(II)	Base Activated carbon	37.9	(Hou et al. 2013)
	Na-Montmorillonite	8.4	(Zhu et al. 2011)
	Chitosan-PAA-Montmorillonite	174	(Yan et al. 2012)
	Fe_3O_4-chitosan	35.5	(Yuwei and Jianlong 2011)
	Fe_3O_4-chitosan films	123.4	(Lasheen et al. 2016)
	This work	229.6	
Ni(II)	Activated carbon	44.1	(Ewecharoen et al. 2009)
	Na-Montmorillonite	46	(Barati et al. 2013)
	Chitosan-PAA	435	(Wang and Kuo 2008)
	Fe_3O_4-chitosan	52.6	(Tran et al. 2010)
	Fe_3O_4-chitosan films	109.8	(Lasheen et al. 2016)
	This work	108.9	

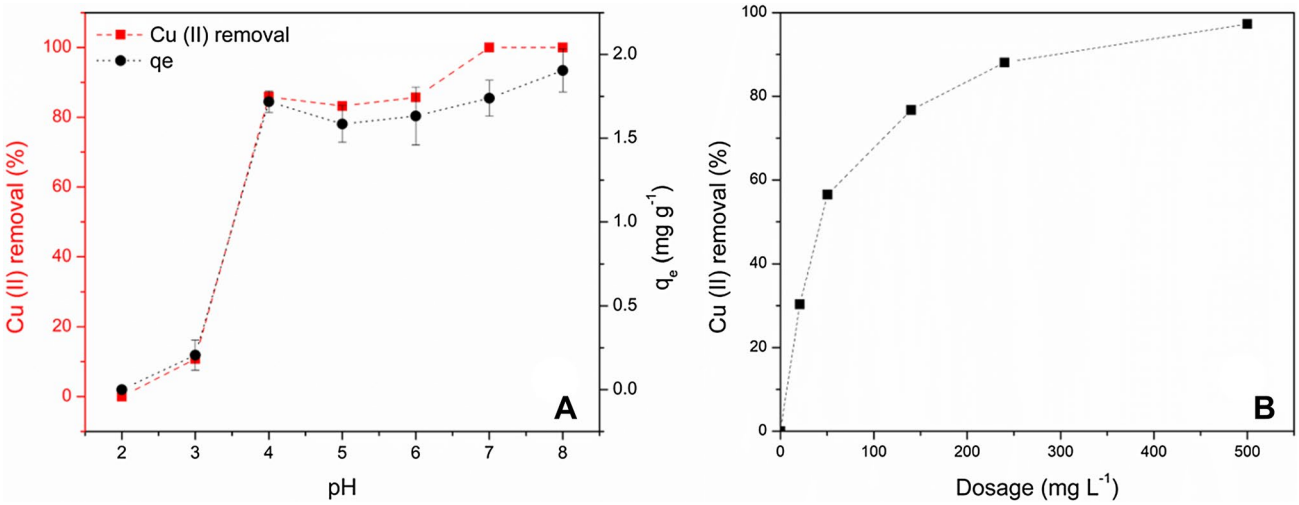

Fig. 5 **a** Effect of pH on the % removal and adsorption capacity of Cu(II) on MCC. $[Cu(II)]_0 = 1$ mg L^{-1}, [MCC] = 500 mg L^{-1}, contact time = 3 h. **b** Effect of adsorbent dosage on Cu (II) removal. $[Cu(II)]_0 = 2$ mg L^{-1}, pH = 6, contact time = 3 h

organic ligands) and others cationic species with the adsorbents could takes place, limiting the interaction between the heavy metal and the adsorbent. Furthermore, constituents of natural waters, such as dissolved organic matter (DOM), may block the active sites of the adsorbent materials (Liu et al. 2008). For this reason, the effects of both DOM and Ca(II) ion on the uptake of Cu(II) were evaluated. Cu(II) adsorption experiments in presence of humic acids (HA) (1–6 mg L^{-1}) and Ca(II) (0.0001–0.1 M), carried out separately, were performed (Fig. 6a). A significant drop of Cu(II) removal to 30 mg g^{-1} occurred with the addition of Ca(II) up to 0.1 M. This can be attributed to the high complexation capacity of MCC with Ca(II) ions. In contrast, in the presence of HA, the uptake of Cu(II) is increased showing a complex behavior. Increase of HA concentration from 0 to 2 mg L^{-1} enhanced the uptake, while further addition of HA results in a slight decrease of Cu(II) removals. The comparison between the recorded UV–Vis spectra of an aqueous solution of HA and the supernatant of the magnetic separated dispersion of MCC in the presence of Cu(II) ions and HA (Fig. S8, in the Online Resource), showed that HA is completely retained by the MCC in the concentration range studied. Thus, the increased MCC adsorption capacity in the presence of HA is probably due to additional active sites for adsorption of heavy metals provided by the adsorbed HA. It is well-known that HA exhibits strong affinities toward metal ions due to a large number of ionisable functional groups, which are mainly carboxylic and phenolic groups (Hernández et al. 2006; Terbouche et al. 2010). The slight decrease of the Cu(II) uptake observed at HA concentration higher

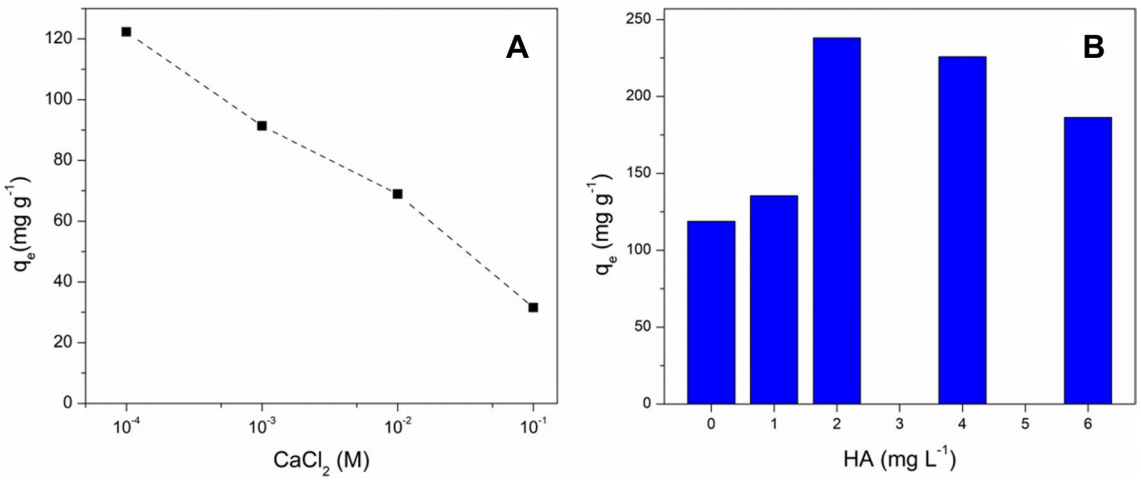

Fig. 6 Effect of Ca(II) (**a**) and HA concentration (**b**) on Cu(II) removal. $[Cu(II)]_0 = 8$ mg L^{-1}, [MCC] = 50 mg L^{-1}, pH = 6, contact time = 3 h

than 2 mg L^{-1}, could be correlated to adsorbed HA hindering the active surface sites of MCC, however, the Cu(II) uptake was still higher than in the absence of HA.

The Cu(II) removal during seven continuous cycles of regeneration and reuse is shown in Fig. 7. No loss of Cu(II) adsorption capacity was observed on the regenerated MCC after six cycles, whereas in the last (7^{th}) cycle, MCC retained about 60% of the initial removal capacity. The reusability of the adsorbent is one of the most important features for its application in wastewater treatments, thus, the great performance shown by the material in recovery and reuse cycles encourages the design of continuous MCC-based flow-through systems for water treatments with high heavy metals removal efficiency.

4 Conclusions

Results reported in this paper show the potential applicability of magnetic chitosan composites (MCC) for the removal of heavy metals in wastewater treatments. MCC showed an excellent ability to remove Cu(II), Pb(II) and Ni(II) from water. Characterization of the adsorption behaviour revealed that kinetics and isotherms were best fitted by the pseudo-second-order model and the Langmuir isotherm model, respectively. The results exhibited extremely high removal capacity towards Cu(II) and Pb(II). Adsorption experiments at different pH evidenced that the application of MCC is limited at pH values lower than four, probably due to chitosan solubilisation in the acidic environment. On the other hand, MCC showed the advantage of being easily separated from the aqueous media by the application of an external magnetic field, recovered after washing step with an acid aqueous solution and reused up to six cycles.

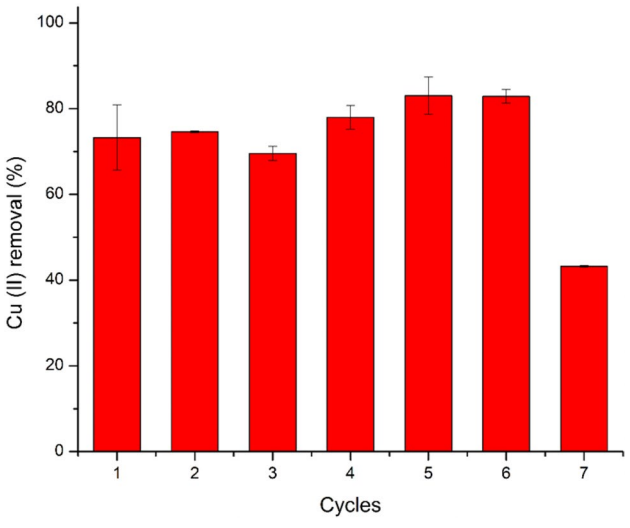

Fig. 7 Cycles of reuse (adsorption shown) of MCC in the removal of Cu(II). $[Cu(II)]_0 = 2$ mg L^{-1}, [MCC] = 250 mg L^{-1}, pH = 6, contact time = 3 h

Acknowledgement The present work was partially supported by UNCo (PIP 04/I217) and CONICET (PIP 12-2013-01-00236CO). This project has received funding from the European Union's Horizon 2020 research and innovation programme under the Maria Sklodowska-Curie grant agreement No 645551 (Mat4Treat). M.E. Peralta thank the CONICET for his research graduate grant.

References

Ahmad, R., Mirza, A.: Application of Xanthan gum/n-acetyl cysteine modified mica bionanocomposite as an adsorbent for the removal of toxic heavy metals. Groundw. Sustain. Dev. **7**, 101–108 (2018). https://doi.org/10.1016/j.gsd.2018.03.010

Arias, J.L., Reddy, L.H., Couvreur, P.: Fe3O4/chitosan nanocomposite for magnetic drug targeting to cancer. J. Mater. Chem. **22**, 7622 (2012). https://doi.org/10.1039/c2jm15339d

Azzam, E.M.S., Eshaq, G., Rabie, A.M., Bakr, A.A., Abd-Elaal, A.A., El Metwally, A.E., Tawfik, S.M.: Preparation and characterization of chitosan-clay nanocomposites for the removal of Cu(II) from aqueous solution. Int. J. Biol. Macromol. **89**, 507–517 (2016). https://doi.org/10.1016/j.ijbiomac.2016.05.004

Babel, S.: Low-cost adsorbents for heavy metals uptake from contaminated water: a review. J. Hazard. Mater. **97**, 219–243 (2003). https://doi.org/10.1016/S0304-3894(02)00263-7

Barati, A., Asgari, M., Miri, T., Eskandari, Z.: Removal and recovery of copper and nickel ions from aqueous solution by poly(methacrylamide-co-acrylic acid)/montmorillonite nanocomposites. Environ. Sci. Pollut. Res. **20**, 6242–6255 (2013). https://doi.org/10.1007/s11356-013-1672-3

Boddu, V.M., Abburi, K., Talbott, J.L., Smith, E.D., Haasch, R.: Removal of arsenic (III) and arsenic (V) from aqueous medium using chitosan-coated biosorbent. Water Res. **42**, 633–642 (2008). https://doi.org/10.1016/j.watres.2007.08.014

Cesano, F., Fenoglio, G., Carlos, L., Nisticò, R.: One-step synthesis of magnetic chitosan polymer composite films. Appl. Surf. Sci. **345**, 175–181 (2015). https://doi.org/10.1016/j.apsusc.2015.03.154

Chang, Y.C., Chen, D.H.: Preparation and adsorption properties of monodisperse chitosan-bound Fe3O4 magnetic nanoparticles for removal of Cu(II) ions. J. Colloid Interface Sci. **283**, 446–451 (2005). https://doi.org/10.1016/j.jcis.2004.09.010

Cho, D.W., Jeon, B.H., Chon, C.M., Kim, Y., Schwartz, F.W., Lee, E.S., Song, H.: A novel chitosan/clay/magnetite composite for adsorption of Cu(II) and As(V). Chem. Eng. J. **200–202**, 654–662 (2012). https://doi.org/10.1016/j.cej.2012.06.126

Corazzari, I., Nisticò, R., Turci, F., Faga, M.G., Franzoso, F., Tabasso, S., Magnacca, G.: Advanced physico-chemical characterization of chitosan by means of TGA coupled on-line with FTIR and GCMS: thermal degradation and water adsorption capacity. Polym. Degrad. Stab. **112**, 1–9 (2015). https://doi.org/10.1016/j.polymdegradstab.2014.12.006

Dragan, E.S., Loghin, D.F.A.: Fabrication and characterization of composite cryobeads based on chitosan and starches-g-PAN as efficient and reusable biosorbents for removal of Cu2+, Ni2+, and Co2+ions. Int. J. Biol. Macromol. **120**, 1872–1883 (2018). https://doi.org/10.1016/j.ijbiomac.2018.10.007

Ewecharoen, A., Thiravetyan, P., Wendel, E., Bertagnolli, H.: Nickel adsorption by sodium polyacrylate-grafted activated carbon. J. Hazard. Mater. **171**, 335–339 (2009). https://doi.org/10.1016/J.JHAZMAT.2009.06.008

Gao, J., He, Y., Zhao, X., Ran, X., Wu, Y., Su, Y., Dai, J.: Single step synthesis of amine-functionalized mesoporous magnetite nanoparticles and their application for copper ions removal from aqueous solution. J. Colloid Interface Sci. **481**, 220–228 (2016). https://doi.org/10.1016/j.jcis.2016.07.057

Hernández, D., Plaza, C., Senesi, N., Polo, A.: Detection of Copper(II) and zinc(II) binding to humic acids from pig slurry and amended soils by fluorescence spectroscopy. Environ. Pollut. **143**, 212–220 (2006). https://doi.org/10.1016/j.envpol.2005.11.038

Ho, Y.S.: Review of second-order models for adsorption systems. J. Hazard. Mater. **136**, 681–689 (2006). https://doi.org/10.1016/j.jhazmat.2005.12.043

Horst, M.F., Alvarez, M., Lassalle, V.L.: Removal of heavy metals from wastewater using magnetic nanocomposites: analysis of the experimental conditions. Sep. Sci. Technol. **51**, 550–563 (2016). https://doi.org/10.1080/01496395.2015.1086801

Hou, X.-X., Deng, Q.-F., Ren, T.-Z., Yuan, Z.-Y.: Adsorption of Cu2 + and methyl orange from aqueous solutions by activated carbons of corncob-derived char wastes. Environ. Sci. Pollut. Res. **20**, 8521–8534 (2013). https://doi.org/10.1007/s11356-013-1792-9

Ibrahim, A.G., Saleh, A.S., Elsharma, E.M., Metwally, E., Siyam, T.: Chitosan-g-maleic acid for effective removal of copper and nickel ions from their solutions. Int. J. Biol. Macromol. **121**, 1287–1294 (2019). https://doi.org/10.1016/j.ijbiomac.2018.10.107

Jin, X., Li, K., Ning, P., Bao, S., Tang, L.: Removal of Cu(II) ions from aqueous solution by magnetic chitosan-tripolyphosphate modified silica-coated adsorbent: characterization and mechanisms. Water, Air, Soil Pollut **228**, 302 (2017). https://doi.org/10.1007/s11270-017-3482-6

Kim, D.K., Mikhaylova, M., Zhang, Y., Muhammed, M.: Protective coating of superparamagnetic iron oxide nanoparticles. Chem. Mater. **15**, 1617–1627 (2003). https://doi.org/10.1021/cm021349j

Kongarapu, R.J., Nayak, A.K., Khobragade, M.U., Pal, A.: Surfactant bilayer on chitosan bead surface for enhanced Ni(II) adsorption. Sustain. Mater. Technol. **18**, e00077 (2018). https://doi.org/10.1016/j.susmat.2018.e00077

Lasheen, M.R., El-Sherif, I.Y., Tawfik, M.E., El-Wakeel, S.T., El-Shahat, M.F.: Preparation and adsorption properties of nano magnetite chitosan films for heavy metal ions from aqueous solution. Mater. Res. Bull. **80**, 344–350 (2016). https://doi.org/10.1016/j.materresbull.2016.04.011

Laus, R., Costa, T.G., Szpoganicz, B., Fávere, V.T.: Adsorption and desorption of Cu(II), Cd(II) and Pb(II) ions using chitosan crosslinked with epichlorohydrin-triphosphate as the adsorbent. J. Hazard. Mater. **183**, 233–241 (2010). https://doi.org/10.1016/j.jhazmat.2010.07.016

Li, G.Y., Jiang, Y.R., Huang, K.L., Ding, P., Chen, J.: Preparation and properties of magnetic Fe3O4-chitosan nanoparticles. J. Alloys Compd **466**, 451–456 (2008). https://doi.org/10.1016/j.jallcom.2007.11.100

Li, H., Bi, S., Liu, L., Dong, W., Wang, X.: Separation and accumulation of Cu(II), Zn(II) and Cr(VI) from aqueous solution by magnetic chitosan modified with diethylenetriamine. Desalination **278**, 397–404 (2011). https://doi.org/10.1016/j.desal.2011.05.056

Li, K., Li, P., Cai, J., Xiao, S., Yang, H., Li, A.: Efficient adsorption of both methyl orange and chromium from their aqueous mixtures using a quaternary ammonium salt modified chitosan magnetic composite adsorbent. Chemosphere **154**, 310–318 (2016). https://doi.org/10.1016/j.chemosphere.2016.03.100

Li, X., Zhou, H., Wu, W., Wei, S., Xu, Y., Kuang, Y.: Studies of heavy metal ion adsorption on Chitosan/Sulfydryl-functionalized graphene oxide composites. J. Colloid Interface Sci. **448**, 389–397 (2015). https://doi.org/10.1016/j.jcis.2015.02.039

Liang, X., Duan, J., Xu, Q., Wei, X., Lu, A., Zhang, L.: Ampholytic microspheres constructed from chitosan and carrageenan in alkali/urea aqueous solution for purification of various wastewater. Chem. Eng. J. **317**, 766–776 (2017). https://doi.org/10.1016/j.cej.2017.02.089

Lin, J.-C., SenGupta, A.K.: Hybrid anion exchange fibers with dual binding sites: simultaneous and reversible sorption of perchlorate and arsenate. Environ. Eng. Sci. **26**, 1673–1683 (2009). https://doi.org/10.1089/ees.2009.0170

Liu, J., Zhao, Z., Jiang, G.: Coating Fe_3O_4 magnetic nanoparticles with humic acid for high efficient removal of heavy metals in water. Environ. Sci. Technol. **42**, 6949–6954 (2008). https://doi.org/10.1021/es800924c

Liu, Y.: New insights into pseudo-second-order kinetic equation for adsorption. Colloids Surfaces A Physicochem. Eng. Asp. **320**, 275–278 (2008). https://doi.org/10.1016/j.colsurfa.2008.01.032

Magnacca, G., Allera, A., Montoneri, E., Celi, L., Benito, D.E., Gagliardi, L.G., Carlos, L.: Novel magnetite nanoparticles coated with waste sourced bio- based substances as sustainable and renewable adsorbing materials. ACS Sustain. Chem. Eng. **2**, 1518–1524 (2014). https://doi.org/10.1021/sc500213j

Mano, J.F., Koniarova, D., Reis, R.L.: Thermal properties of thermoplastic starch/synthetic polymer blends with potential biomedical applicability. J. Mater. Sci. **14**, 127–135 (2003)

Martín-Lara, M.A., Blázquez, G., Calero, M., Almendros, A.I., Ronda, A.: Binary biosorption of copper and lead onto pine cone shell in batch reactors and in fixed bed columns. Int. J. Miner. Process. **148**, 72–82 (2016). https://doi.org/10.1016/j.minpro.2016.01.017

Modin, H., Persson, K.M., Andersson, A., van Praagh, M.: Removal of metals from landfill leachate by sorption to activated carbon, bone meal and iron fines. J. Hazard. Mater. **189**, 749–754 (2011). https://doi.org/10.1016/j.jhazmat.2011.03.001

Mokhtari, M., Keshtkar, A.R.: Removal of Th(IV), Ni(II)and Fe(II) from aqueous solutions by a novel PAN–TiO2 nanofiber adsorbent modified with aminopropyltriethoxysilane. Res. Chem. Intermed. **42**, 4055–4076 (2016). https://doi.org/10.1007/s11164-015-2258-0

Mouni, L., Merabet, D., Bouzaza, A., Belkhiri, L.: Adsorption of Pb(II) from aqueous solutions using activated carbon developed from Apricot stone. Desalination **276**, 148–153 (2011). https://doi.org/10.1016/j.desal.2011.03.038

Musso, T.B., Parolo, M.E., Pettinari, G., Francisca, F.M.: Cu(II) and Zn(II) adsorption capacity of three different clay liner materials. J. Environ. Manage. **146**, 50–58 (2014). https://doi.org/10.1016/j.jenvman.2014.07.026

Neeraj, G., Krishnan, S., Senthil Kumar, P., Shriaishvarya, K.R., Vinoth Kumar, V.: Performance study on sequestration of copper ions from contaminated water using newly synthesized high effective chitosan coated magnetic nanoparticles. J. Mol. Liq. **214**, 335–346 (2016). https://doi.org/10.1016/j.molliq.2015.11.051

Nguyen, M.L., Huang, C., Juang, R.-S.: Synergistic biosorption between phenol and nickel(II) from Binary mixtures on chemically and biologically modified chitosan beads. Chem. Eng. J. **286**, 68–75 (2016). https://doi.org/10.1016/J.CEJ.2015.10.065

Nisticò, R.: Aquatic-derived biomaterials for a sustainable future: a European opportunity. Resources **6**, 65 (2017a). https://doi.org/10.3390/resources6040065

Nisticò, R.: Magnetic materials and water treatments for a sustainable future. Res. Chem. Intermed **43**, 6911–6949 (2017b). https://doi.org/10.1007/s11164-017-3029-x

Nisticò, R., Celi, L.R., Bianco Prevot, A., Carlos, L., Magnacca, G., Zanzo, E., Martin, M.: Sustainable magnet-responsive nanomaterials for the removal of arsenic from contaminated water. J. Hazard. Mater. **342**, 260–269 (2018). https://doi.org/10.1016/j.jhazmat.2017.08.034

Nisticò, R., Franzoso, F., Cesano, F., Scarano, D., Magnacca, G., Parolo, M.E., Carlos, L.: Chitosan-derived iron oxide systems for magnetically guided and efficient water purification processes from polycyclic aromatic hydrocarbons. ACS Sustain. Chem. Eng.

5, 793–801 (2017). https://doi.org/10.1021/acssuschemeng.6b02126

Owsianiak, M., Veltman, K., Hauschild, M.Z., Hendriks, A.J., Steinmann, Z.J.N., Huijbregts, M.A.J.: Elucidating differences in metal absorption efficiencies between terrestrial soft-bodied and aquatic species. Chemosphere **112**, 487–495 (2014). https://doi.org/10.1016/j.chemosphere.2014.05.024

Qiu, H., Lv, L., Pan, B., Zhang, Q., Zhang, W., Zhang, Q.: Critical review in adsorption kinetic models. J. Zhejiang Univ. A. **10**, 716–724 (2009). https://doi.org/10.1631/jzus.A0820524

Su, C.: Environmental implications and applications of engineered nanoscale magnetite and its hybrid nanocomposites: a review of recent literature. J. Hazard. Mater. **322**, 48–84 (2017). https://doi.org/10.1016/j.jhazmat.2016.06.060

Terbouche, A., Djebbar, S., Benali-Baitich, O., Bouet, G.: Characterization and complexing capacity of humic acid extracted from yakouren soil with heavy metals by conductimetry and quenching of fluorescence. Soil Sediment Contam. **19**, 21–41 (2010). https://doi.org/10.1080/15320380903401724

Tran, H.V., Tran, L.D., Nguyen, T.N.: Preparation of chitosan/magnetite composite beads and their application for removal of Pb(II) and Ni(II) from aqueous solution. Mater. Sci. Eng., C **30**, 304–310 (2010). https://doi.org/10.1016/j.msec.2009.11.008

USEPA: The Analysis of Occurrence Data from the Unregulated Contaminant Monitoring Program (UCM) and National Inorganics and Radionuclides Survey (NIRS) in Support of Regulatory Determinations for the Second Drinking Water Contaminant Candidate List (CCL 2) EPA. (2008)

Wang, J.-W., Kuo, Y.-M.: Preparation and adsorption properties of chitosan–poly(acrylic acid) nanoparticles for the removal of nickel ions. J. Appl. Polym. Sci. **107**, 2333–2342 (2008). https://doi.org/10.1002/app.27247

Wang, S., Wang, K., Dai, C., Shi, H., Li, J.: Adsorption of Pb2 + on amino-functionalized core–shell magnetic mesoporous SBA-15 silica composite. Chem. Eng. J. **262**, 897–903 (2015). https://doi.org/10.1016/J.CEJ.2014.10.035

Wang, X., Wang, C.: Chitosan-poly(vinyl alcohol)/attapulgite nanocomposites for copper(II) ions removal: pH dependence and adsorption mechanisms. Colloids Surfaces A Physicochem. Eng. Asp. **500**, 186–194 (2016). https://doi.org/10.1016/j.colsurfa.2016.04.034

World Health Organization: Guidelines for drinking-water quality: FOURTH EDITION. (2011). https://doi.org/10.1016/s1462-0758(00)00006-6

Yan, H., Yang, L., Yang, Z., Yang, H., Li, A., Cheng, R.: Preparation of chitosan/poly(acrylic acid) magnetic composite microspheres and applications in the removal of copper(II) ions from aqueous solutions. J. Hazard. Mater. **229–230**, 371–380 (2012). https://doi.org/10.1016/J.JHAZMAT.2012.06.014

Yang, H., Sheikhi, A., van de Ven, T.G.M.: Reusable green aerogels from cross-linked hairy nanocrystalline cellulose and modified chitosan for dye removal. Langmuir **32**, 11771–11779 (2016). https://doi.org/10.1021/acs.langmuir.6b03084

You, L., Huang, C., Lu, F., Wang, A., Liu, X., Zhang, Q.: Facile synthesis of high performance porous magnetic chitosan - polyethylenimine polymer composite for Congo red removal. Int. J. Biol. Macromol. **107**, 1620–1628 (2018). https://doi.org/10.1016/j.ijbiomac.2017.10.025

Yuwei, C., Jianlong, W.: Preparation and characterization of magnetic chitosan nanoparticles and its application for Cu(II) removal. Chem. Eng. J. **168**, 286–292 (2011). https://doi.org/10.1016/j.cej.2011.01.006

Zhang, M., Zhou, Q., Li, A., Shuang, C., Wang, W., Wang, M.: A magnetic sorbent for the efficient and rapid extraction of organic micropollutants from large-volume environmental water samples. J. Chromatogr. A **1316**, 44–52 (2013). https://doi.org/10.1016/j.chroma.2013.09.086

Zhu, J., Cozzolino, V., Pigna, M., Huang, Q., Caporale, A.G., Violante, A.: Sorption of Cu, Pb and Cr on Na-montmorillonite: competition and effect of major elements. Chemosphere **84**, 484–489 (2011). https://doi.org/10.1016/j.chemosphere.2011.03.020

Zhu, Y., Hu, J., Wang, J.: Competitive adsorption of Pb(II), Cu(II) and Zn(II) onto xanthate-modified magnetic chitosan. J. Hazard. Mater. **221–222**, 155–161 (2012). https://doi.org/10.1016/J.JHAZMAT.2012.04.026